Magnetic Field Effects on Intramolecular Exciplex Fluorescence of Chain-Linked Phenanthrene and *N*,*N*-Dimethylaniline: Influence of Chain Length, Solvent, and Temperature

Hong Cao, Yoshihisa Fujiwara, Takeharu Haino, Yoshimasa Fukazawa, Chen-Ho Tung,# and Yoshifumi Tanimoto*

Department of Chemistry, Faculty of Science, Hiroshima University, Kagamiyama, Higashi-Hiroshima 739

(Received April 26, 1996)

Magnetic field effects (MFEs) on the intramolecular exciplex fluorescence of a chain-linked phenanthrene (Phen)/*N*,*N*-dimethylaniline (DMA) system, Phen–$(CH_2)_n$–O–$(CH_2)_2$–DMA, have been studied in the magnetic fields ($\leq$0.62 T) as functions of (1) solvent polarity (ε = 7.6—36.7), (2) chain length (n = 4—12), and (3) temperature (223—333 K). The MFEs on the exciplex fluorescence are attributable to the singlet–triplet intersystem crossing in the intramolecular radical ion pair which is in dynamic equilibrium with the exciplex. (1) Solvent polarity increases significantly the MFEs on the exciplex fluorescence of Phen–$(CH_2)_{10}$–O–$(CH_2)_2$–DMA. This is attributable to the stability of the intramolecular radical ion pair relative to the exciplex. (2) A remarkable influence of chain length on MFEs in the exciplex fluorescence in *N*,*N*-dimethylformamide (DMF) was observed. The results were discussed in connection with the edge-to-edge distances $\langle r \rangle$ of two radicals obtained from molecular dynamics calculation for model compounds. (3) The temperature-induced high-field shift of the exchange energies $|2J|$ for Phen–$(CH_2)_4$–O–$(CH_2)_2$–DMA in DMF was discussed in connection with $\langle r \rangle$.

Magnetic field effects (MFEs) on photochemical and photophysical processes have been studied extensively in recent years.[1] Study of exciplex fluorescence in a magnetic field may provide us important information on dynamics of short-lived singlet radical ion pairs which are strongly coupled with the exciplexes. Especially, fluorescence measurements are suitable means for precise consideration of the effects, since their accuracy and sensitivity are much higher than those of transient absorption measurements. MFEs on exciplex fluorescence have been studied by a few groups.[2—6] MFEs on the intermolecular exciplex fluorescence of pyrene (Py)/*N*,*N*-dimethylaniline (DMA) have been reported by Petrov et al.[2] and Batchelor et al.[3] The effects on the intramolecular exciplex fluorescence of chain-linked Py/DMA (Py–$(CH_2)_n$–DMA) and related compounds, in addition to the effects on the T–T absorption of Py, have been studied very extensively by Weller, Staerk and their collaborators.[4] Exciplex fluorescence of polymers containing Py and DMA in solution has been reported by Chowdhury et al.[5] Tanimoto and his collaborators have studied the MFEs on the intramolecular exciplex fluorescence of polymethylene chain-linked phenanthrene (Phen)/*N*,*N*-dimethylaniline (DMA) (Phen–$(CH_2)_n$–DMA, n = 3—10) and copolymers containing Phen and DMA moieties as well as the intermolecular Phen/DMA in solution.[6]

The MFEs on the exciplex fluorescence of the chain-linked system, Phen–$(CH_2)_n$–DMA, are different from those for the intermolecular Py/DMA system as discussed in a previous paper.[6] For example, the dependence of the MFEs on solvent polarity is remarkably different in these two systems. In the case of Phen–$(CH_2)_{10}$–DMA, the magnitude of the MFE on the exciplex fluorescence intensity increases monotonously by increasing solvent polarity in the range of 7.6 (tetrahydrofuran) to 35.9 (acetonitrile), whereas for the intermolecular Py/DMA system a maximum of the MFE appears at ε = ca. 20.[2] This maximum is called the medium dielectric constant (mDK) MFE maximum.[4f] This phenomenon has been considered to arise from the competition between the singlet–triplet intersystem crossing of the radical ion pair and the dissociation of the pair in the intermolecular system. Since radical ion pairs linked by covalent bonds can not dissociate, the mDK maximum is not expected to appear in the intramolecular system, as was the case of Phen–$(CH_2)_{10}$–DMA. However, very recently it was reported that the exciplex fluorescence from Py–$(CH_2)_n$–DMA (n=9,16) exhibits the mDK MFE maximum.[4f] Consequently MFEs on the two chain-linked systems are different from each other.

In a previous work, the MFEs have been examined for the biradicals generated from Phen–$(CH_2)_n$–DMA of short and medium chain lengths (n = 3—10), in which energies of two radical ion states are non-degenerate, and the results were discussed in a qualitative manner. It is the purpose of the present paper to unravel the mechanisms of the MFEs on the singlet biradicals precisely and quantitatively. New chain-

Permanent address: Institute of Photographic Chemistry, Chinese Academy of Sciences, Beijing 100101, China.

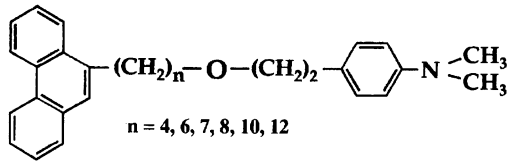

Phen-n-O-2-DMA

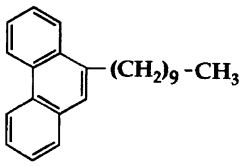

Phen-10

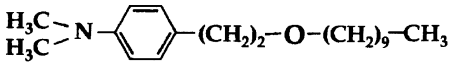

DMA-2-O-10

Chart 1.

linked Phen/DMA compounds (Phen-*n*-O-2-DMA, Chart 1), which are suitable for the present purpose, were synthesized and the MFEs on the exciplex fluorescence from them were studied by means of photostationary and time-resolved fluorescence spectroscopies as well as transient absorption one. Influence of solvent polarity, chain length and temperature on the MFEs were examined. Molecular dynamics calculation was carried out for the model compounds so we could discuss the influence of edge-to-edge distances of two radicals on the observed MFEs quantitatively.

Experimental

Materials. 2-[4-(Dimethylamino)phenyl]ethyl ω-(9-Phenanthryl)alkyl Ether (Phen-*n*-O-2-DMA): 2-[4-(Dimethylamino)phenyl]ethyl 10-(9-phenanthryl)decyl ether (Phen-10-O-2-DMA) was synthesized by the following procedure. To an anhydrous diethyl ether solution (20 ml) of 2.6 g 9-bromophenanthrene in a flask in an ice bath, a 15% hexane solution (12 ml) of butyllithium was added dropwise and then the mixture was stirred for 4 h. To this mixture was added 7 ml of 1,10-dibromodecane at once. After stirring for several minutes, the flask was placed in an oil bath and the solution was refluxed for 2 h. The reaction mixture was extracted by benzene. The benzene layer was washed with water and saturated NaCl aqueous solution and then dried over Na_2SO_4 overnight. The benzene was evaporated. The residue was purified by column chromatography on silica (Wako, C-200, hexane), giving 2.0 g of 1-(9-phenanthryl)-10-bromodecane (Phen-10-Br, 50% yield) as a white solid.

Phen-10-Br (1.8 g) and 1.6 g of 2-[(4-dimethylamino)phenyl]-ethanol (Aldrich) were added to a solution (20 ml) of 1.5 g of NaH (abt. 60% oil suspension) in *N*,*N*-dimethylacetamide and this was stirred for 4 h in an ice bath. The reaction mixture was filtered and extracted by benzene. The benzene layer was washed with ice water and saturated NaCl aqueous solution, and then dried over Na_2SO_4 overnight. The product was separated by column chromatography on silica (Wako, C-200) with hexane–chloroform (2 : 1) as eluent to give a crude solid. It was purified by recrystallization from hexane to afford Phen-10-O-2-DMA as white crystals (400 mg, 18% yield). Mp 49—50 °C. ^{1}H NMR ($CDCl_3$, 270 MHz) δ = 8.76—7.56 (d, 9H protons of phenanthrene ring), 7.11—6.67 (d, 4H protons of benzene ring), 3.59—3.40 (t, 4H O–CH_2), 3.14—3.08 (t, 2H –CH_2–DMA), 2.90 (6H, –CH_3), 2.82—2.77 (t, 2H Phen–CH_2), 1.84—1.29 (t, 16H protons of chain). IR (KBr) 2924, 2850, 1468, (–$(CH_2)_n$–) 1616, 1523, ($\phi_{C=C}$) 1348, (C–N) 1117, (C–O–C) 949, 880, 809, 770, 741, 721 cm^{-1}. MS (EI) *m*/*z* 481 (M^+; 100), 191 (Phen–CH_2; 85), 134 (CH_2 – DMA, 100). Anal. Calcd for $C_{34}H_{43}NO$: C, 84.77; H, 9.00; N, 2.91%. Found: C, 84.88; H, 9.15; N, 2.79%.

Other ethers with different chain lengths (Phen-*n*-O-2-DMA, *n* = 4,6,7,8,12), 9-decylphenanthrene (Phen-10), and 2-[4-(dimethylamino)phenyl]ethyl decyl ether (DMA-2-O-10) were prepared in an analogous manner.

For spectroscopic measurements, spectrograde *N*,*N*-dimethylformamide (DMF), acetonitrile (MeCN), tetrahydrofuran (THF), and dimethyl sulfoxide (DMSO) were used as received. The concentrations of all samples were about 10^{-4} mol dm^{-3}. All solutions were deaerated by several freeze-pump-thaw cycles.

Apparatus. The conventional fluorescence and absorption spectra were measured with a Hitachi F-3010 fluorescence spectrophotometer and a U-3210 spectrophotometer, respectively. Fluorescence decay curves were measured with an excimer laser (Lumonics 500, 308 nm) as an exciting light source and a 10 cm monochromator (Ritsu, MC-10L)–photomultiplier (Hamamatsu, R928)–digital oscilloscope (Tektronix, 2440)–microcomputer (NEC, PC-9801) as an detection system. Transient absorption spectra were measured with the experimental setup mentioned above where a xenon arc lamp (Ushio, UXL-500-O) was used as the probe light source.[7)]

The photostationary fluorescence spectra in the presence of a magnetic field were measured with the fluorescence spectrophotometer mentioned above by attaching a permanent magnet (ca. 0.26 T).

The photostationary fluorescence intensities in the presence of magnetic fields were determined by using a super-high-pressure Hg lamp (Ushio, USH-500D) equipped with a narrow band-path filter (Melles Greot, 03FIU004, 300 nm, FWHM 10 nm) as an exciting light source and a filter (Melles Greot, 03FIV006, 500 nm, FWHM 10 nm)–photomultiplier (Hamamatsu, R928)–chart recorder (Graphtec, SR6211) as a detection system. An electromagnet (Tokin, SEE-9) was used in the above measurements. The time-resolved fluorescence and transient absorption measurements in magnetic fields were also performed on the above setup. Its residual field was < 0.5 mT by applying an electric current for cancellation. The magnetic field strength was determined by a gaussmeter (Denshijiki, GM-1220).

Analysis of Fluorescence Lifetime. The decay curves of exciplex fluorescence could not be always expressed by a single exponential. The exciplex fluorescence decay for short chain molecules was analyzed by single exponential fittings, while for longer chain molecules in a polar solvent double exponential fittings were used:

$$I(t) = C_1 \exp(-t/\tau_1) + C_2 \exp(-t/\tau_2), \quad (1)$$

where $I(t)$ is the fluorescence intensity at time t, τ_1, and τ_2 are the lifetimes of the fast and slow decay components, respectively,

and C_1 and C_2 are the respective pre-exponential factors. When fluorescence decay was double exponential, a mean lifetime $\langle\tau\rangle$ was used as described by Werner et al.[4e,f] which was calculated according to:

$$\langle\tau\rangle = (C_1\tau_1 + C_2\tau_2)/(C_1 + C_2). \quad (2)$$

Molecular Dynamics Calculation. Estimation of the mean edge-to-edge distance $\langle r\rangle$ of the two radical ion pairs was performed for model compounds, *n*-alkyl propyl ethers, CH_3–$(CH_2)_{n-1}$–O–$(CH_2)_2$–CH_3 ($n = 5$—13), and CH_3–$(CH_2)_{10}$–CH_3 by the mixed Monte Carlo/stochastic dynamics (MC/SD) method using the Macro Model v.4.5 program.[8,9] The AMBER* force field was employed for the simulation with the GB/SA water solvation model.[10] The total simulation time was 1000 ps with a 1.5 fs time step for the SD calculation. The first 50 ps of the each simulation was taken as an equilibration period. The MC part of the calculation used random rotations of all rotatable bonds. The ratio of SD steps to MC steps was one to one. Nonbonded cutoff distances were not used. Structures were sampled every 1 ps for 1000 ps. The mean distance between the methyl carbon atoms at the two ends was evaluated from those sampled structures as a representative of the edge-to-edge distance in the radical ion pair.

Results

1. Phen-10-O-2-DMA in DMF. 1.1 Assignment of Fluorescence Spectrum: Figure 1 shows the absorption spectra of Phen-10-O-2-DMA, Phen-10, and DMA-2-O-10 in DMF. Making a comparison with the absorption spectra of Phen-10 and DMA-2-O-10, the absorption band of Phen-10-O-2-DMA at 330—350 nm is chiefly attributable to the absorption band of Phen and the band at 290—320 nm is attributable to the sum of absorption bands of Phen and DMA. The ratios of the molecular extinction coefficients of Phen to DMA are 4 : 1 at 300 nm and 1 : 3 at 308 nm.

Influence of the excitation wavelength on the fluorescence spectra of Phen-10-O-2-DMA is shown in Fig. 2. The spectra in the 340—450 nm region are considerably affected by the excitation wavelength, whereas the broad band peaked at ca. 500 nm is independent of the excitation wavelength. Taking into account the spectra of Phen-10 and DMA-2-O-10 shown

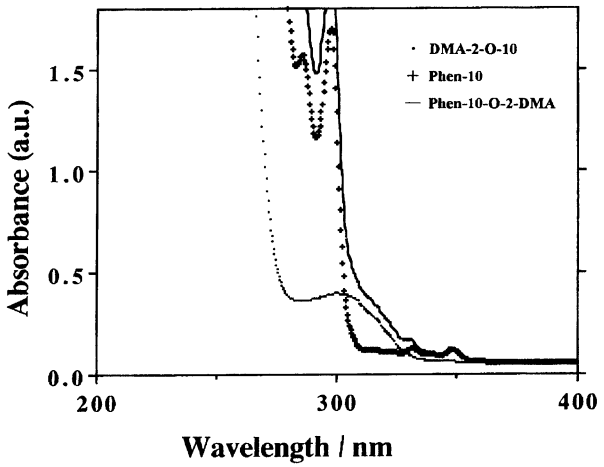

Fig. 1. Absorption spectra of Phen-10-O-2-DMA, Phen-10, and DMA-2-O-10 in DMF.

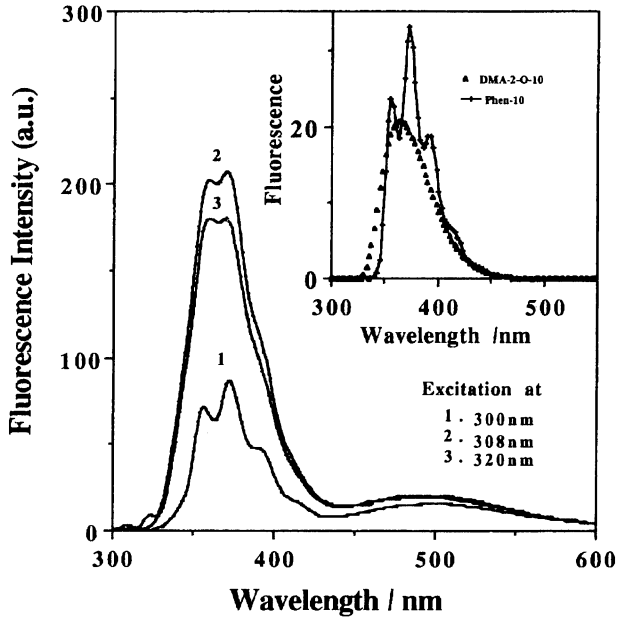

Fig. 2. Influence of excitation wavelength on the fluorescence spectra of Phen-10-O-2-DMA in DMF. Inset: Fluorescence spectra of Phen-10 and DMA-2-O-10 in DMF. Excitation wavelength is 308 nm.

in the inset, the fluorescence bands in the 350—450 nm region are attributable to the sum of the fluorescence of the Phen and the DMA moieties. When excited at 300 nm, the 370 nm band is mainly attributable to the fluorescence of ^{1}Phen*, whereas it is the mixture of those of ^{1}Phen* and ^{1}DMA* when excited at 308 nm. The broad band around 500 nm is assigned to the singlet exciplex generated by the intramolecular electron transfer from DMA to ^{1}Phen*, as will be discussed later.

To make the assignment clearly, the fluorescence decay at 370 nm was examined for Phen-10, DMA-2-O-10, and Phen-10-O-2-DMA in DMF. The lifetimes of Phen-10 and DMA-2-O-10 are 48 and 6 ns, respectively, whereas that of Phen-10-O-2-DMA monitored at 370 nm is ca. 5 ns, though fluorescence from two moieties were not separated. Fluorescence from the ^{1}Phen* moiety is strongly quenched in the presence of the DMA moiety. The quenching of ^{1}DMA* is insignificant, if any, as the lifetimes of the excited DMA are the same order of magnitude for DMA-2-O-10 and Phen-10-O-2-DMA. These facts indicate that the exciplex is mainly generated from ^{1}Phen* and not from ^{1}DMA*.

1.2 Magnetic Field Effects on the Fluorescence and Transient Absorption of Phen-10-O-2-DMA in DMF:

Photostationary Fluorescence Spectrum: Figure 3 shows the MFE on the fluorescence spectra of Phen-10-O-2-DMA in DMF. In the presence of a magnetic field (0.26 T), the fluorescence intensity of the exciplex peaked at 500 nm increases significantly, whereas that of the 370 nm band is independent of the magnetic field. Magnetic field-induced enhancement in the exciplex fluorescence intensity is about 2.2 times, which is independent of the excitation wavelength between 300 and 350 nm.

Time-Resolved Fluorescence Spectra: The time-resolved fluorescence spectra, taken by the 308 nm laser excitation, are shown in Fig. 4. The fluorescence of ^{1}Phen* and ^{1}DMA* in the 350—400 nm region disappears at ca. 30 ns after the laser pulse, leaving a long-lived exciplex fluorescence in the 450—550 nm region. The fluorescence intensity of the exciplex (500 nm) observed at 70 ns delay increases 2—3 times in the presence of a magnetic field (0.35 T), whereas the 370 nm band is insensitive to the magnetic field. The mean lifetimes of the exciplex are 29 ns (0 T) and 70 ns (0.38 T). These observations are in line with the results from Fig. 3.

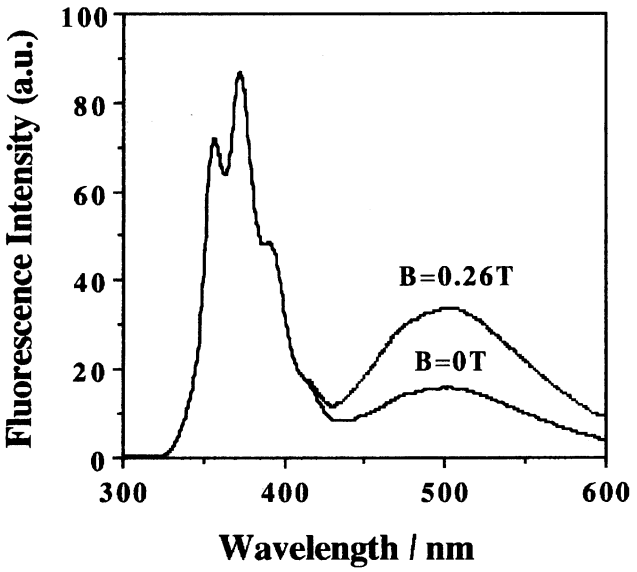

Fig. 3. Magnetic field effect on the fluorescence of Phen-10-O-2-DMA in DMF. Excitation wavelength is 300 nm.

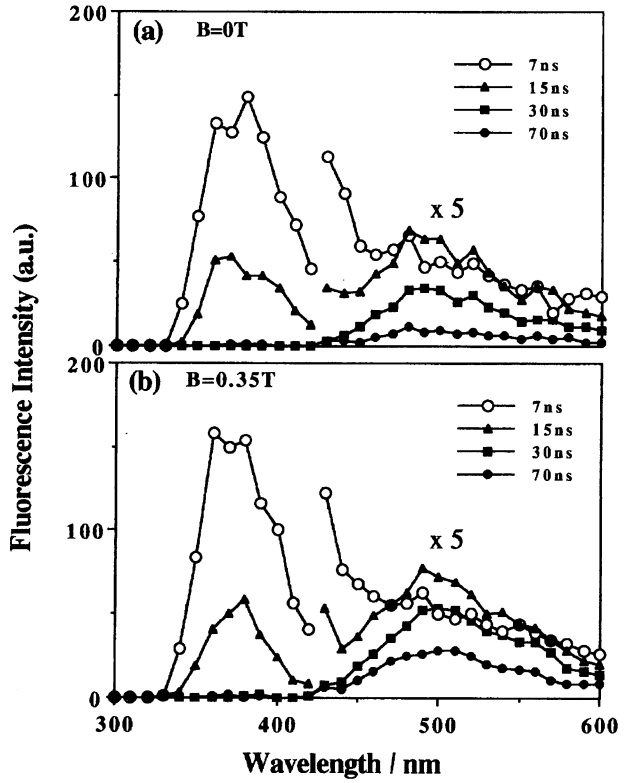

Fig. 4. Time-resolved fluorescence spectra of Phen-10-O-2-DMA in DMF. Excitation wavelength is 308 nm.

Transient Absorption Spectra: Transient absorption spectra of Phen-10-O-2-DMA in DMF appear in the 400—500 nm region (Fig. 5). As shown in the inset, a short-lived transient absorption of ^{2}Phen$^-$ appears at 400—430 nm immediately after the laser excitation,[11] though the absorption in the longer wavelength region was contaminated by the intense fluorescence at the delay times shorter than ca. 100 ns. This indicates the formation of an exciplex and/or a radical ion pair in the reaction. Making a comparison with the absorption spectra of Phen-10 and DMA-2-O-10 in DMF, the absorption band at 460—490 nm, appearing at 0.3 μs delay, is assigned chiefly to the triplet–triplet absorption of Phen, the contribution of the T–T band of DMA being minor in this region, if any. Lifetimes of transient absorption of ^{2}Phen$^-$ and ^{3}Phen* are about 29 ns and 3.5 μs, respectively.

Figure 6 shows the MFE on the decay of transient absorption of Phen-10-O-2-DMA observed at 430 nm. The short-lived component due to ^{2}Phen$^-$ is significantly affected by the magnetic field, though the long-lived one due to ^{3}Phen* is independent of the field within the experimental error. It seems that ^{3}Phen* is mainly generated directly from ^{1}Phen*. The lifetimes of ^{2}Phen$^-$ are 29 ns (0 T) and 80 ns (0.36 T), respectively, which are in good agreement with those determined from the exciplex fluorescence decay. Analogously, the lifetimes of ^{2}Phen$^-$ in Phen-12-O-2-DMA were found to be 21 (0 T) and 71 ns (0.36 T) in DMF. The MFE on the transient absorption mentioned above indicates that a radical ion pair (RIP) of ^{2}Phen$^-$ and ^{2}DMA$^+$ has intervened in the reaction.

1.3 Influence of Solvent Polarity:

Photostationary Fluorescence: Many investigators have explored the yield of RIP as a function of solvent po-

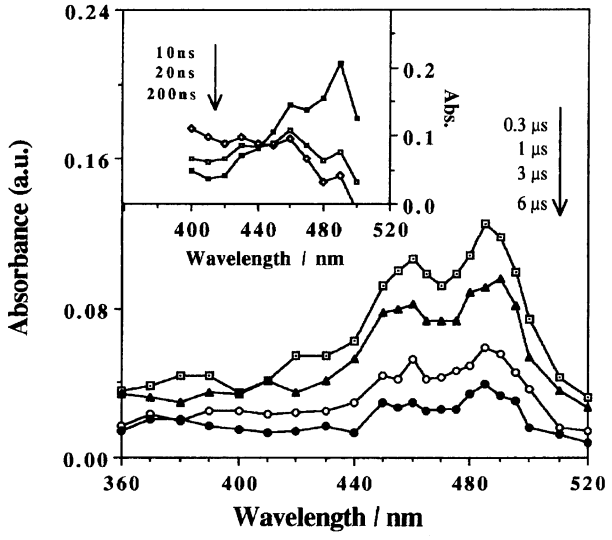

Fig. 5. Transient absorption spectra of Phen-10-O-2-DMA in DMF. Excitation wavelength is 308 nm. Inset: Transient spectra at short delay times.

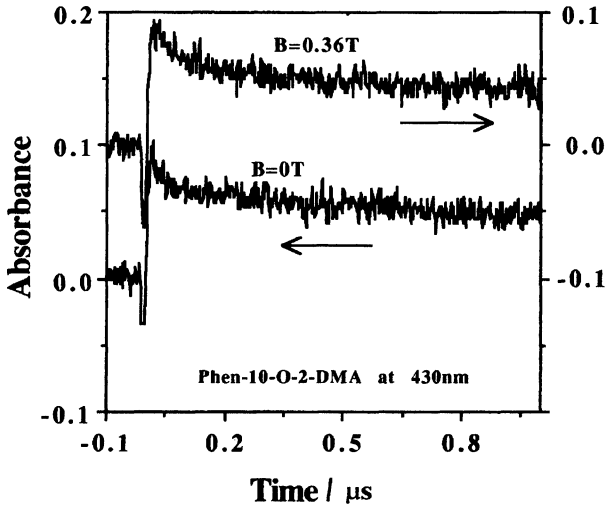

Fig. 6. Magnetic field effect on the decay of the transient absorption of Phen-10-O-2-DMA observed at 430 nm.

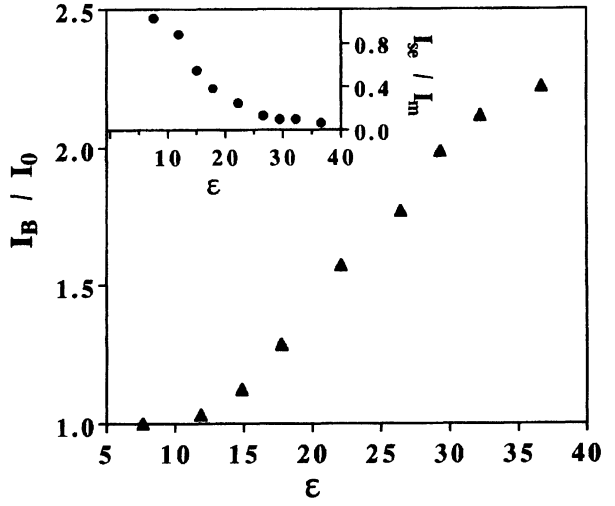

Fig. 7. Influence of solvent polarity on the magnetic field effects on the exciplex fluorescence intensities of Phen-10-O-2-DMA observed at 500 nm. I_0 and I_B are intensities in the absence and presence of a magnetic field (0.26 T), respectively. Inset: Influence of solvent polarity on the ratio of the fluorescence intensities observed at 500 nm (I_{se}) and 370 nm (I_m).

larity. Here, the influence of solvent polarity upon the MFE of the exciplex fluorescence intensity of Phen-10-O-2-DMA was examined. Figure 7 shows the influence of solvent polarity on the photostationary intensity ratio I_B/I_0 of the exciplex fluorescence, I_B and I_0 being the intensities in the presence and absence of a magnetic field of 0.26 T, respectively. The intensity ratio I_{se}/I_m of the exciplex band (500 nm) to the 370 nm band is also displayed in the inset. In THF (ε=7.6) an external magnetic field does not affect the exciplex fluorescence intensity at all. For solvents with higher dielectric constants the MFE on the intensity ratio becomes significant and the ratio becomes as large as 2.3 at ε=37, whereas the relative yield I_{se}/I_m of the exciplex decreases significantly.

Fluorescence Lifetime: The magnetic field effects on the lifetime of exciplex fluorescence in solvents with different polarity were studied in detail for Phen-10-O-2-DMA. The results are summarized in Fig. 8 and Table 1. The lifetimes of the 370 nm band are ca. 5 ns and are magnetic field independent in all the solvents used. Exciplex fluorescence lifetimes both in the presence and absence of a magnetic field (0.57 T) are strongly dependent on the solvent polarity. In THF the lifetime is about 48 ns and magnetic-field-independent. In DMF the fluorescence decay curve becomes double exponential and the mean lifetimes are about 28 ns at zero field and about 70 ns at 0.57 T. The magnetic field dependence (MFD) of the lifetime are parallel with that of photostationary intensity shown in Fig. 7.

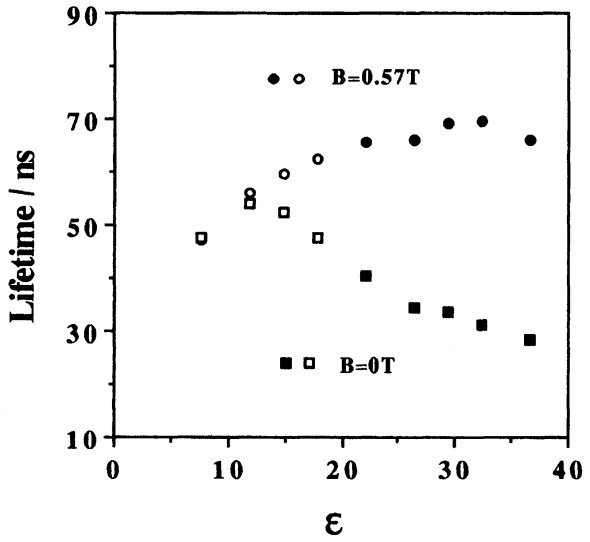

Fig. 8. Influence of solvent polarity on the exciplex fluorescence lifetime of Phen-10-O-2-DMA in the absence and presence of a magnetic field (0.57 T). □ and ○ are the lifetime in the absence and presence of a magnetic field (0.57 T), respectively. ■ and ● are the mean lifetime $\langle\tau\rangle$ in the absence and presence of a magnetic field (0.57 T), respectively. See text.

It is interesting to note that the MFE on the exciplex lifetime is larger in DMF than in MeCN, though the ε values of the two solvents are similar. In this case, solvent viscosity seems to affect the MFE considerably. The MFE in DMSO is slightly smaller than that in DMF. This might be attributable to the hydrogen bonding in DMSO, since in the case of Phen–$(CH_2)_{10}$–DMA the MFEs in alcohol are always smaller than those in aprotic mixed solvents with similar polarity.[6)]

2. Magnetic Field Effects on the Exciplex Fluorescence of Phen-*n*-O-2-DMA in DMF. 2.1 Photostationary Fluorescence: Influence of chain length on the MFEs was examined in DMF in which the most significant effect is observed for the fluorescence of Phen-10-O-2-DMA. The bifunctional chain-linked molecules Phen-*n*-O-2-DMA with n=4,6,7,8,12 exhibit the exciplex fluorescence in almost the same wavelength region as that of Phen-10-O-2-DMA (Fig. 2). Figure 9 shows the MFD of exciplex fluorescence intensity ratio I_B/I_0 of Phen-*n*-O-2-DMA in DMF, I_B and I_0 be-

Table 1. Influence of Dielectric Constant (ε) and Viscosity (η/cP) of Solvent on the Fluorescence Lifetimes of Phen-10-O-2-DMA in the Absence and Presence of a Magnetic Field (0.57 T)

Solvent	ε	η	τ/ns (0 T)		τ/ns (0.57 T)	
			370 nm[a)]	500 nm[a)]	370 nm[a)]	500 nm[a)]
DMSO	46.7	1.996	5.8	18.8[c)]	5.8	44.4[c)]
MeCN	35.9	0.345	3.5	44.6[c)]	3.5	70.8[c)]
DMF	36.7	0.924	5.1	28.3[c)]	5.3	65.8[c)]
85%DMF+15%THF	32.3[b)]	—	5.4	31.2[c)]	5.1	69.5[c)]
75%DMF+25%THF	29.4[b)]	—	5.4	33.4[c)]	5.2	69.3[c)]
65%DMF+35%THF	26.5[b)]	—	5.0	34.4[c)]	5.3	65.9[c)]
50%DMF+50%THF	22.1[b)]	—	5.1	40.2[c)]	5.3	65.6[c)]
35%DMF+65%THF	17.8[b)]	—	5.3	47.7	5.3	62.4
25%DMF+75%THF	14.9[b)]	—	5.4	52.3	5.5	59.8
15%DMF+85%THF	11.9[b)]	—	5.5	53.8	5.2	55.9
THF	7.58	0.550	5.8	47.7	5.9	47.3

a) Wavelength for fluorescence decay measurements. b) Calculated from equation $\varepsilon_{mix}=\varepsilon_{DMF}v_1+\varepsilon_{THF}v_2$, where v_i is the volume fraction of solvent i. c) Mean lifetime $\langle\tau\rangle$.

ing the intensities in the presence and absence of a magnetic field B. The intensity ratio I_{se}/I_m of the exciplex fluorescence to the monomer one is also displayed in the inset. With increasing n from 4 to 12, the ratio I_B/I_0 at B=0.35—0.59 T increases drastically, though the relative yield of exciplex fluorescence I_{se}/I_m decreases. When n is small (n=4,6,7), the dips of the ratio are clearly observed. The magnetic fields, at which the ratios become their respective minimum, are 180 (n=4), 30 (n=6), 11 (n=7), and 7.7 mT (n=8). When n=12, the magnetic field-induced increase in the ratio I_B/I_0 is about 2.4 at 0.59 T. This is the most significant effect on the exciplex fluorescence intensity so far reported.

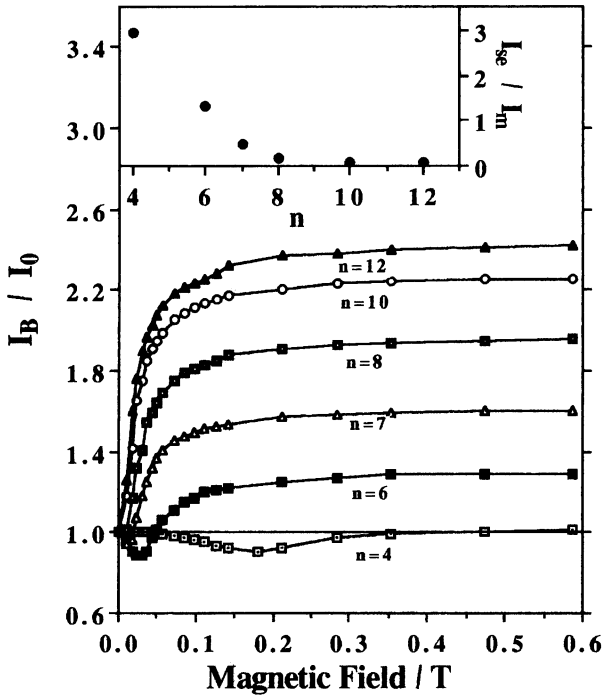

Fig. 9. Magnetic field dependence of the exciplex fluorescence intensities of Phen-n-O-2-DMA in DMF. I_0 and I_B are intensities in the absence and presence of a magnetic field B, respectively. Inset: Influence of the chain length n on the ratio of the fluorescence intensities observed at 500 nm (I_{se}) and 370 nm (I_m).

2.2 Fluorescence Lifetime: The MFD of the fluorescence lifetimes of the exciplex generated from Phen-n-O-2-DMA in DMF are presented in Fig. 10 and Table 2. The lifetimes exhibit significant MFEs, especially when n is large. In the case of the exciplexes with n=4 and 6, shallow dips

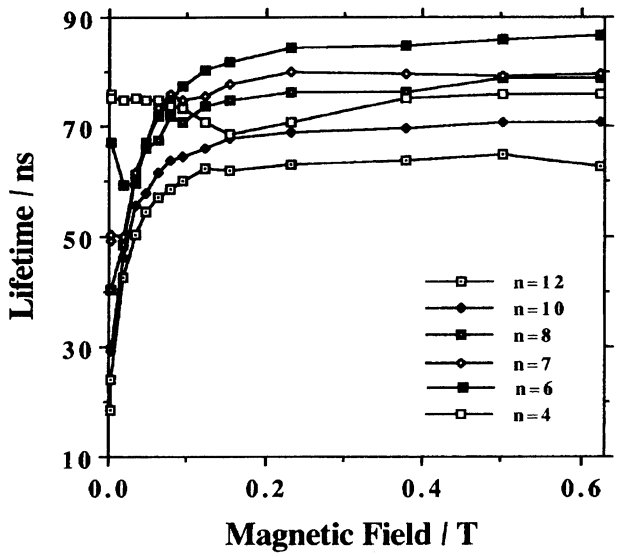

Fig. 10. Magnetic field dependence of the exciplex fluorescence lifetimes of Phen-n-O-2-DMA in DMF. Lifetimes for compounds with n=10,12 are the mean lifetimes $\langle\tau\rangle$. See text.

Table 2. Exciplex Fluorescence Lifetime of Phen-n-O-2-DMA in DMF in the Absence and Presence of a Magnetic Field (0.62 T).

n	4	6	7	8	10	12
τ(0 T)/ns	75.2	67.2	50.3[a)]	40.2[a)]	29.3[a)]	21.3[a)]
τ(0.62 T)/ns	76.1	86.7	79.8[a)]	78.9[a)]	70.9[a)]	62.5[a)]

a) Mean lifetime $\langle\tau\rangle$.

are also observed, as in the case of the MFD of the exciplex fluorescence intensity mentioned above.

2.3 Temperature Dependence of MFE: Figure 11 shows the influence of temperature on the photostationary fluorescence intensity ratio I_B/I_0 for Phen-*n*-O-2-DMA (*n*=4, 6,7) in DMF. In the case of Phen-4-O-2-DMA, the minimum is 112 mT at 220 K and moves gradually to the higher field by increasing temperature, the minimum being 209 mT at 336 K. Analogous change is also observed for the exciplexes with *n*=6 and 7. As shown in Fig. 12, the minima shift linearly to higher fields in the temperature region between 217 and 341 K, though their slopes are dependent on *n*.

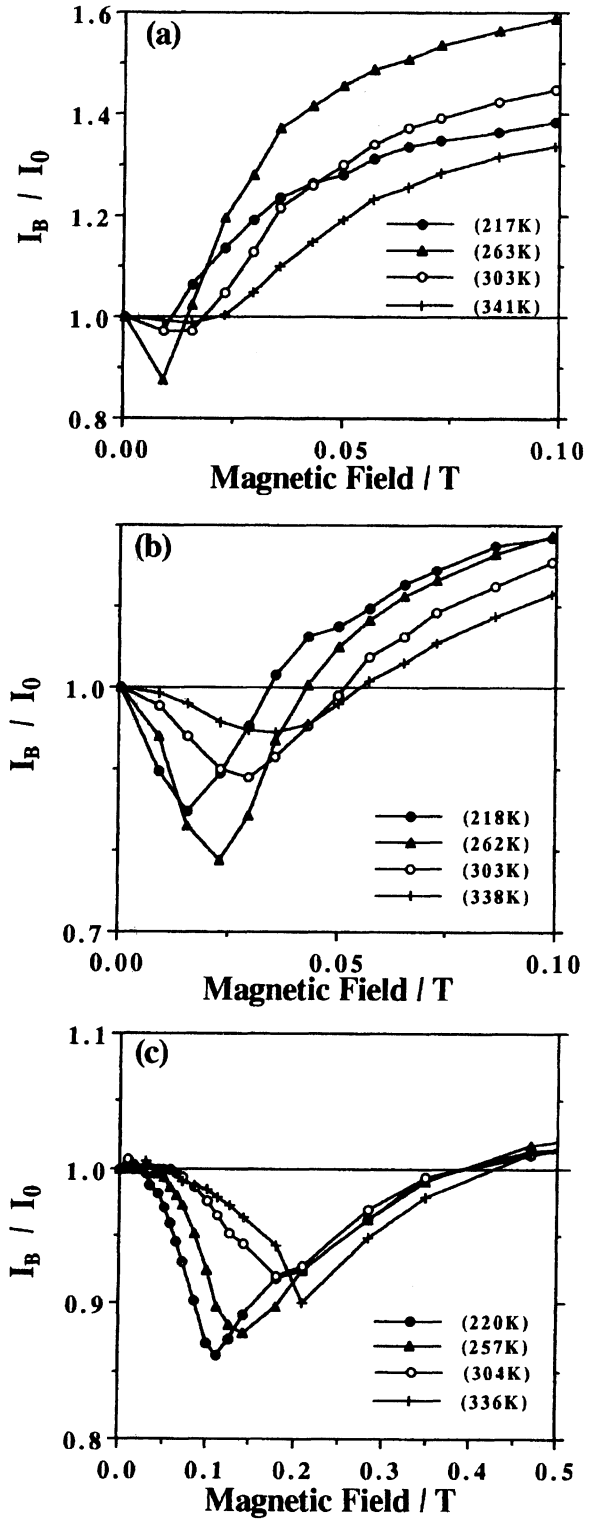

Fig. 11. Influence of temperature on the magnetic field dependence of exciplex fluorescence of Phen-*n*-O-2-DMA (*n*=4,6,7) in DMF. (a) *n*=7, (b) *n*=6, and (c) *n*=4.

Discussion

1. Magnetic Field Effects on the Exciplex Fluorescence of Phen-10-O-2-DMA. 1.1 Reaction Scheme and Mechanism of MFE: Taking into account absorption and photostationary fluorescence spectra, and time-resolved fluorescence and transient absorption ones shown in Figs. 1, 2, 3, 4, 5, and 6, the primary processes in the photochemical reaction of the present system in DMF are proposed, as shown in Scheme 1. After photoexcitation, ^{1}Phen* is generated. End-to-end electron-transfer reaction between ^{1}Phen* and DMA leads to the formation of an intramolecular singlet radical ion pair (SRIP). Singlet exciplex (SE) is generated from SRIP. SRIP undergoes intersystem crossing (ISC) to the triplet radical ion pair (TRIP). SE and SRIP are considered to be in fast dynamic equilibrium. The SE-SRIP system can deactivate via three processes: (1) the radiative and nonradiative decay from SE, (2) the back electron transfer in SRIP and (3) the ISC from SRIP to TRIP, as discussed in a previous paper.[6] The MFEs on the SE fluorescence would originate from the effects on the ISC process between SRIP and TRIP, as will be mentioned later.

In DMF, electron transfer seems to be the more efficient process in the intramolecular quenching of ^{1}Phen* by DMA, rather than the direct SE formation, on the basis of the following two reasons. (1) Electron transfer takes place at every end-to-end distance of the chain, whereas SE formation occurs only when ^{1}Phen* and DMA are in close proximity (ca. 3 Å) (1 Å=0.1 nm). Thus, the frequency of electron transfer is considered to be much higher than that of the SE formation. (2) In DMF, the free energy change ($-\Delta G$) for

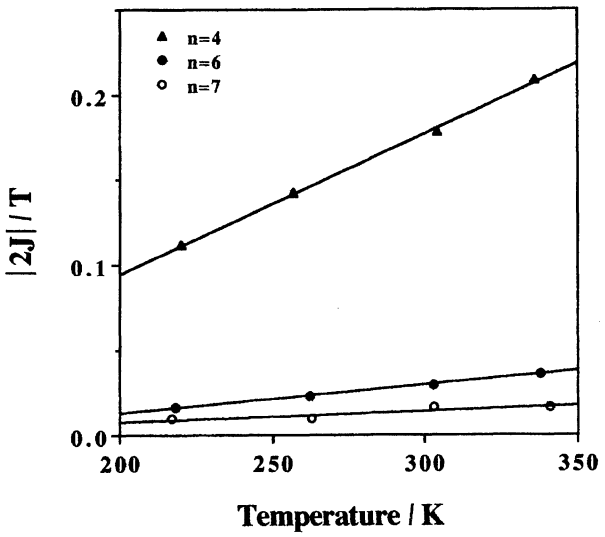

Fig. 12. Plot of |2*J*| vs. temperature.

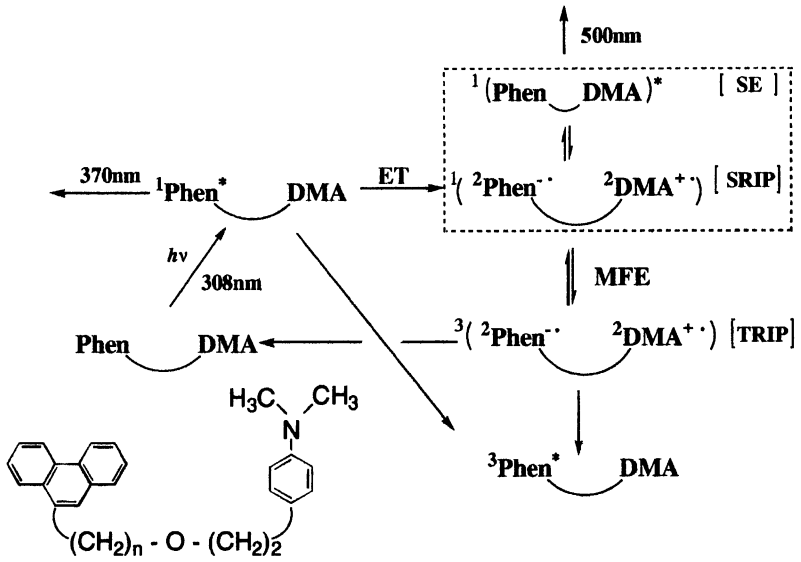

Scheme 1.

the SRIP formation is larger than that for the SE formation, since SRIP is more stable in energy than SE (see, Section 1.2 of Discussion).

In a previous paper, we have studied the exciplex fluorescence of Phen–$(CH_2)_{10}$–DMA in MeCN.[6] The exciplex is also generated from ^{1}DMA*, in addition to that from ^{1}Phen*. In the present case, ^{1}DMA* does not seem to form an exciplex. The molecular conformation of the present chain molecule containing an ether oxygen atom seems slightly different from that of Phen–$(CH_2)_{10}$–DMA in which the two moieties are linked by a pure polymethylene chain.

In the case of Phen-10-O-2-DMA, significant MFEs are observed for its exciplex fluorescence intensity and lifetime (Figs. 3 and 4) as well as the decay of transient absorption (Fig. 6). These MFEs can be explained by the radical pair mechanism. In this molecule, SE and SRIP are considered to be in fast dynamic equilibrium. The SE-SRIP may deactivate partly through the S–T ISC process in RIP. At zero field the electron-nuclear hyperfine (hf)–induced ISC occurs between the nearly degenerate three triplet sublevels (T_+, T_0, T_-) and the singlet state (S) in RIPs. In the presence of a magnetic field (>ca. 0.2 T), the ISCs between the two triplet sublevels (T_+, T_-) and S are restrained because of the Zeeman splitting of T_+ and T_- (hf mechanism), as will be discussed in detail later.

1.2 Influence of Solvent Polarity: Influence of solvent polarity on the MFE is strongly correlated to the stability of RIP relative to exciplex. The energies (ΔG_{SE}, ΔG_{RIP}) of exciplex and RIP are calculated by using the following equations:[12]

$$\Delta G_{SE} = E_D^{ox} - E_A^{red} + (U_{dest} - U_{stab}) - (\mu^2/\rho^3)[(\varepsilon_s - 1)/(2\varepsilon_s + 1) - 0.19] + 0.38, \quad \text{(eV)}, \quad (3)$$

$$\Delta G_{RIP} = E_D^{ox} - E_A^{red} - 7.2(1/r_D + 1/r_A)(1/37 - 1/\varepsilon_s) - 14.4/(\varepsilon_s d_{cc}), \quad \text{(eV)}, \quad (4)$$

where E_D^{ox} is the half-wave oxidation potential of the donor, D, E_A^{red} is the half-wave reduction potential of the acceptor, A, μ is the dipole moment of the exciplex, ρ is its equivalent sphere radius, ε_s is the dielectric constant of the solvent, U_{dest} and U_{stab} are various destabilizing and stabilizing interactions between the zero-order charge-transfer, nonbonded and locally excited states. The following parameters are used for calculation of ΔG_{SE} and ΔG_{RIP}, for Phen-10-O-2-DMA: E_{DMA}^{ox}=0.81 V in MeCN,[12] E_{Phen}^{red}=−2.20 V in MeCN,[12] $U_{dest}-U_{stab}$=0, μ^2/ρ^3=0.75 eV,[12] r_D=r_A=3 Å, d_{cc}=11.9 Å. The results are shown in Fig. 13.

The energies of exciplex and RIP are almost the same at ε=ca. 10, and, therefore, no significant MFE is observed in the less polar solvent. With increasing the dielectric constant of the solvent, the energy of RIP is stabilized compared with that of the exciplex. At ε=36.7 (DMF) the difference in ΔG is about 0.2 eV (4.6 kcal mol^{-1}). Although this value is considerably larger than the thermal energy at room temperature,

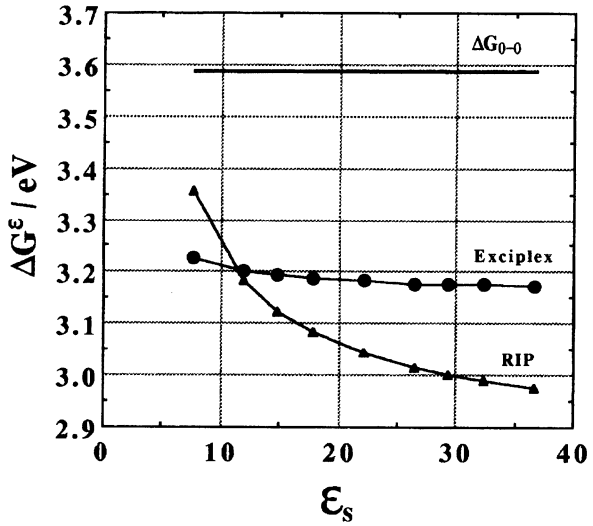

Fig. 13. Influence of solvent polarity on the energies of the intramolecular exciplex, radical ion pair (RIP), and ^{1}Phen*, generated from Phen-10-O-2-DMA.

the above calculation indicates clearly that the equilibrium between SE and SRIP shifts to the latter in a polar solvent, resulting in the significant MFEs in polar solvent. This is in good agreement with the results shown in Figs. 7 and 8.

With increasing solvent polarity, (1) relative intensity of exciplex fluorescence to monomer one decreases, (2) exciplex fluorescence lifetime decreases, (3) the fluorescence decay curve changes from single exponential to double one at ε=ca. 20, and (4) magnitude of the MFE increases. According to the energy diagram shown in Fig. 13, the fraction of RIP which intervenes in the reaction increases with increasing solvent polarity. Since the S–T ISC process in RIP competes with the SE formation process from SRIP, the lifetime of the exciplex fluorescence as well as its intensity should decrease. At zero field, the exciplex fluorescence lifetime decreases from 47.7 ns in THF to 28.3 ns in DMF. This lifetime change is in good agreement with the prediction mentioned above.

Double exponential decay is observed only in polar solvents. This means that double exponential decay is the reflection of dynamics of either (1) the SE-SRIP process or (2) the S–T ISC one of the RIP. In the former case, the rate is considered to be controlled by chain dynamics. Since the difference in solvent viscosity of THF and DMF is not significant (Table 1), it seems unreasonable to consider that the difference in SE-SRIP process affects the SE fluorescence decay. Furthermore, the exciplex fluorescence should exhibit rise and decay instead of double exponential decay, and, therefore (1) is not the case. Based on the following considerations, the S–T spin conversion process (case (2)) seems responsible for the double exponential decay of the exciplex fluorescence. (i) When n is small, the decay is single exponential even in polar solvent. In short chain molecules, degeneracy between singlet and triplet RIP is lifted and S–T spin conversion becomes slow (see, Section 2.1 in Discussion). (ii) The double exponential decay is only observed in the reaction system in which MFEs are significant. Indeed, a study of MFE in higher magnetic field region (1—13 T)[13,14] concluded that the singlet–triplet spin conversion was responsible for the double exponential decay.

Solvent effects on I_B/I_0 shown in Fig. 7 are analogous to those for Phen–$(CH_2)_{10}$–DMA in MeCN.[6] On the other hand, the exciplex fluorescence of Py–$(CH_2)_n$–DMA (n=9, 16) exhibits a medium DK MFE maximum around ε=ca. 20.[4f] In the case of intramolecular exciplexes composed of carbazole (Cz) and methyl hydrogen terephthalate (TP) (Cz–$(CH_2)_n$–TP, n=16—20),[15] their exciplex fluorescence intensities decrease by increasing the solvent polarity from ε=2.2 (dioxane) to 7.6 (THF); with further increasing of the polarity, the fluorescence disappears. At the same time, the lifetime of transient absorption due to the carbazole cation radical, which may be attributable to intramolecular RIP, becomes very short (<20 ns). As a result, MFE was observed for neither exciplex fluorescence nor transient absorption. Comparison of MFEs in the three chain-linked systems indicates that the rates of the magnetic field independent processes from SE and SRIP, which are dependent on solvent polarity, are different in them. As discussed by Werner and Staerk,[4f] the back ET process from SRIP seems to be a most probable candidate for such a process and, therefore, a mDK MFE maximum may be observed under certain conditions.

2. Magnetic Field Effects on Phen-n-O-2-DMA in DMF.

2.1 Influence of Chain Length on MFE: Influence of chain length on the MFEs on the exciplex fluorescence, shown in Figs. 9 and 10, is explained as follows. MFEs caused by the hf mechanism are based on the concept of modifying the mixing between S and T_+, T_0, T_- of RIP, that occurs at zero field or low field and is broken by introducing a Zeeman splitting between the T_0 and the T_+ and T_- states. However in the case of RIP generated by intramolecular ET reaction, the component radicals of the RIP at the ends of the chain cannot separate freely because of the steric restriction imposed by a flexible chain. Its S–T states are nondegenerate even at zero field when a chain length is short. A scalar exchange interaction, $2J$, between the unpaired electrons is supposed to be a parameter controlling the details of the interplay between spin and chain dynamics. The energy gap $|2J|$ of the S–T splitting in RIP is usually expressed in the following form:[16]

$$|2J(r)| = |2J_0| \exp(-\alpha r), \quad (5)$$

where r is the distance of the RIP separation. In the following discussion, $J<0$ is assumed as usual, though a possibility of $J>0$ is suggested for some radical ion pair.[17] The $|2J|$ value increases with the decrease in r, leading to a large S–T separation and a decrease in MFE when r is small. In the case of the molecule with n=4, the S–T separation is quite large compared with other molecules and the observed MFEs are relatively small, as shown in Fig. 9. This is because the $|2J|$ value affects the yield of ISC in RIP as well as the ISC rate in a complex manner.[18] In the case of the molecules with n=10,12, S and T states are nearly degenerate and MFE can be simply explained by the hf mechanism. The (mean) lifetimes of the exciplexes at zero field are 75 (n=4), 67 (n=6), 50 (n=7), 40 (n=8), 29 (n=10), and 21 ns (n=12). Therefore, this lifetime change with n is the reflection of the S–T separation of the respective RIP.

The MFE due to the hf mechanism is usually characterized by the averaged hf interaction, B_{av}, which is calculated from the electron-nuclear hyperfine coupling constants of two component radicals. In the case of (intermolecular) radical pairs composed of pyrene and substituted anilines, this B_{av} value is nearly equal to the magnetic field strength $B_{1/2}$ at which the yield of excited triplet pyrene becomes a half of its saturation value.[4a] In the case of long chain molecules Phen-n-O-2-DMA (n=10,12), the $B_{1/2}$ values, calculated from the MFD of I_B/I_0 shown in Fig. 9, might be comparable with the B_{av} value for the $Phen^-$/DMA^+ pair, since their S and T states are considered to be nearly degenerate. From Fig. 9 the $B_{1/2}$ value is calculated to be about 20 mT. This is about 4 times larger than the B_{av} value (5.5 mT) estimated from the hyperfine coupling constants of component radicals.[6a] As a matter of fact, the MFD of I_B/I_0 is determined not only by

the hf-induced S–T ISC rate but also by the deactivation one from SE-SRIP. In the case of (intermolecular) radical pairs dissociation of the pair also affects the latter rate, whereas it does not take place in that of chain-linked biradicals. This difference in the deactivation rate results in the discrepancy between $B_{1/2}$ and B_{av} in the present molecules.

In the case of short chain biradicals (n=4,6,7), the S–T$_-$ level crossing takes place in low magnetic field and enhances the deactivation of exciplex via S–T$_-$ ISC in RIP, leading to a negative MFE (dips in Fig. 9) (see, Fig. 14). From the dips the $|2J|$values were obtained (Table 3).

Difference in exchange interaction leads to the ISC rate constant (k_{isc}) dependent not only on the magnetic field but also on the chain length which connects the two radicals. If chain length is long, the $|2J|$ is very small and, hence, the k_{isc} should be faster than that of the back electron transfer from TRIP. This leads to a double exponential decay of the exciplex fluorescence when T–S ISC rate is faster than the back ET from TRIP. For a short chain molecule, a large $|2J|$ value decelerates the ISC rate and the rate becomes slower than the rate of deactivation from TRIP. Based on this reason, the exciplex fluorescence decay becomes a single exponential. This is in good agreement with experimental results (Table 2 and Fig. 10).

Distances between the two radicals in a chain-linked biradical are reflected remarkably in the magnitude of MFE, as discussed above. In order to evaluate the distribution of the edge-to-edge distances of Phen and DMA in chain molecules, the MD/stochastic calculation was carried out for $CH_3(CH_2)_n$–O–$(CH_2)_2H_3C$ at 300 K as the models of Phen-n-O-2-DMA. Distances between the two methyl carbon atoms for n=4,7,10 are depicted in Fig. 15. Then the mean distance, $\langle r\rangle$, was also calculated by using the next equation:

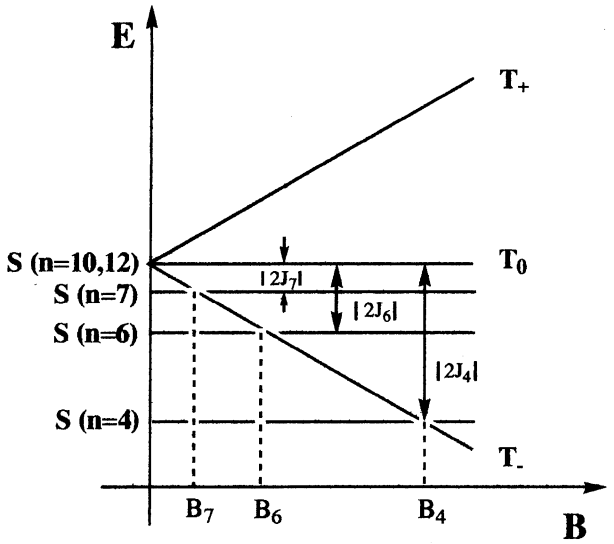

Fig. 14. Schematic energy diagrams of intramolecular radical ion pairs generated from Phen-n-O-2-DMA in magnetic fields. B_n and $|2J_n|$ are the magnetic field strength, where S–T$_-$ level crossing takes place, and the $|2J|$ value for the molecule with chain length n, respectively.

$$\langle r\rangle = \Sigma f_i r_i / \Sigma f_i, \quad (6)$$

where r_i and f_i are the distance between the two methyl carbon atoms and its fraction, respectively. All of the data are summarized in Table 3. From Fig. 15 and Table 3, the following may be derived: With increasing n, interradical edge-to-edge distance increases. The increment of $\langle r\rangle$ per one methylene group is about 0.47 Å. Width of the r_i distribution increases with increasing n. $\langle r\rangle$ for the molecule with n=12 is slightly shorter than that for n=10. This is inconsistent with the MFE shown in Fig. 9. The model used for the present calculation may not be accurate enough to reproduce the $\langle r\rangle$ values for long chain molecules. Because of the hydrophobic interaction between methylene chain and polar solvent, contracted conformations of the chain might be more stable in long chain molecules than in the short chain ones.

The valuable information available from the above-mentioned results is the relationship between $|2J(\langle r\rangle)|$ and $\langle r\rangle$. Here, the $|2J|$ is an average value over all the conformations visited by the linker. In fact, it is possible to compute an energy for each of the many accessible conformations and to obtain an edge-to-edge distance for them. From the plot of $\ln|2J(\langle r\rangle)|$ vs. $\langle r\rangle$ (Fig. 16), the exchange parameters α=1.566 Å^{-1} and $|2J_0|$=4.010×10^8 G (3.52×10^{15} rad s^{-1}) were obtained by Eq. 5.

The α and $|2J_0|$ were estimated to be 2.709 Å^{-1} and 0.892×10^{19} rad s^{-1} from the analysis of CIDNP signals of chain-linked biradicals generated from cyclic ketones.[19] In this case, r is taken to be the center-to-center distance of the two radicals. The difference between the reported values and the present ones may arise from the definition of r, since in the present estimation $\langle r\rangle$ is taken to be the edge-to-edge distance of the two radicals. When a distance of 6 Å is tentatively added to the edge-to-edge distances shown in Table 3 to estimate the center-to-center distances, α and $|2J_0|$ were obtained to be 1.566 Å^{-1} and 4.83×10^{12} G (4.25×10^{19} rad s^{-1}), respectively. Agreement with the CIDNP results seems reasonable, since the $|2J|$ value is an exponential function of r.

Now, let us consider the role of an oxygen atom in the present chain linker. The I_B/I_0 ratio in the exciplex fluorescence of Phen-10-DMA in DMF at 0.75 T is about 1.5,[6] whereas that in the exciplex of Phen-7-O-2-DMA is about 1.6 under the identical conditions. The $|2J|$ values of the former and the latter are 170 G[6] and 110 G, respectively. Although the total number of chain units is the same (10), the MFE is slightly different in the two molecules. The distribution of the distances of the two methyl carbons in $CH_3(CH_2)_{10}CH_3$ was calculated so as to know the influence of the ether oxygen on the chain conformation as a model for Phen–$(CH_2)_{10}$–DMA (Table 3). $\langle r\rangle$ was obtained to be 8.85±2.42 Å. This length is about 0.8 Å shorter than that for CH_3–$(CH_2)_7$–O–$(CH_2)_2$–CH_3 (9.66±2.19 Å). In polar solvent, Phen-10-DMA, having a nonpolar methylene chain, may exist in a closed chain conformation. This situation can be compared with that of the Phen-7-O-2-DMA which has a polar ether oxygen atom at the chain. By introducing an

Table 3. Edge-to-Edge Distance $\langle r \rangle$ and $|2J|$ Values of the Intramolecular Radical Ion Pairs Generated from Phen-*n*-O-2-DMA and Phen-$(CH_2)_{10}$-DMA (1 Å=0.1 nm, 1 Gauss=0.1 mT)
$\langle r \rangle$ are estimated from the average distances between two methyl carbons of CH_3-$(CH_2)_n$-O-$(CH_2)_2$-CH_3 and CH_3-$(CH_2)_{10}$-CH_3. See text.

Sample	Temperature (K)	$\langle r \rangle$/Å	$\|2J\|$/Gauss
	333	7.79±1.15	
Phen-4-O-2-DMA	300	7.88±1.19	1800
	223	8.11±1.19	
Phen-6-O-2-DMA	300	8.97±1.98	302
Phen-7-O-2-DMA	300	9.66±2.19	111
Phen-8-O-2-DMA	300	9.88±2.75	77
Phen-10-O-2-DMA	300	11.93±3.11	3.1[a)]
Phen-12-O-2-DMA	300	11.64±3.46	4.9[a)]
Phen-$(CH_2)_{10}$-DMA	300	8.85±2.42	—

a) Calculated from the equation $|2J|=|2J_0|\exp(-\alpha r)$, where $\alpha=1.566$ Å^{-1} and $|J_0|=2.007\times10^8$ G.

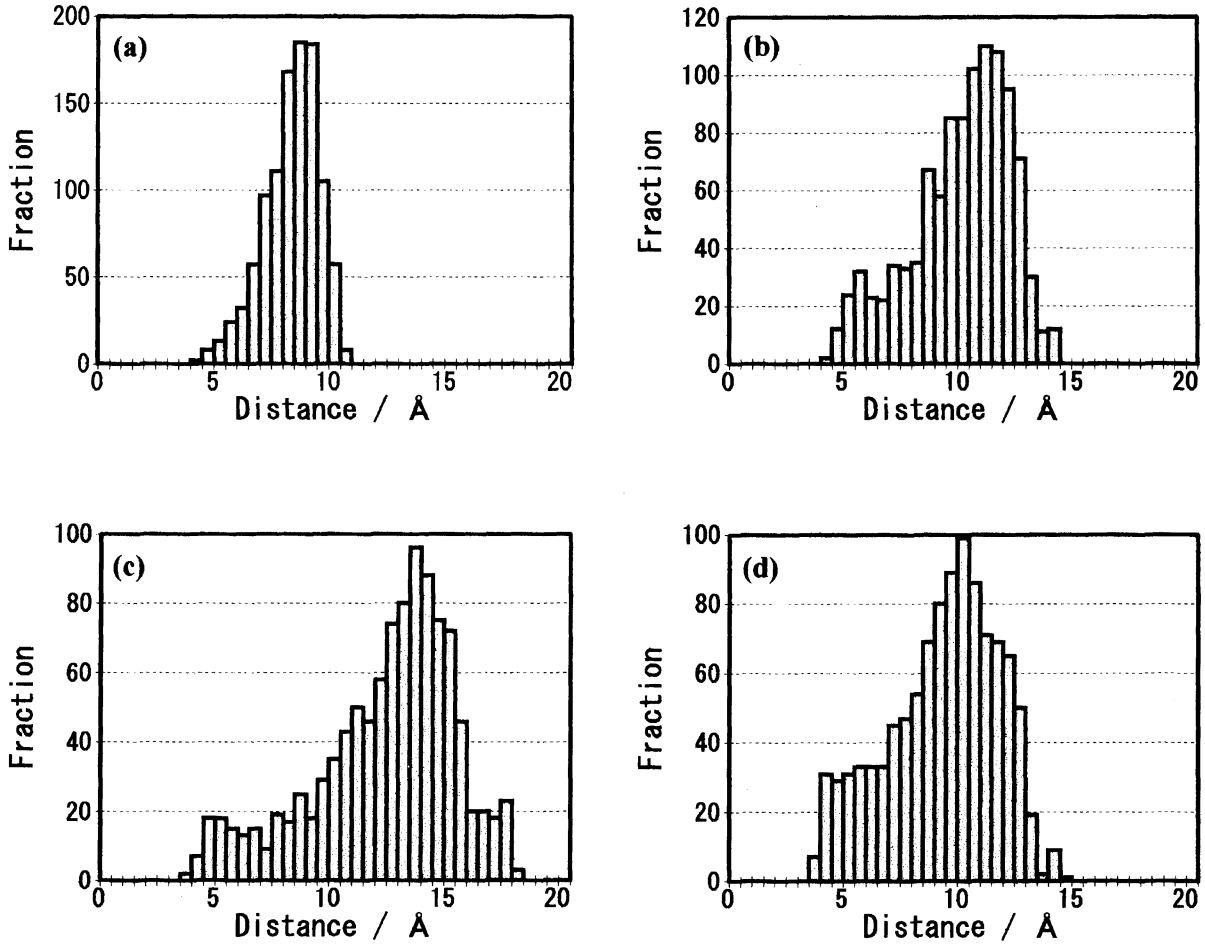

Fig. 15. Distribution of intramolecular distances between two methyl carbon atoms of CH_3-$(CH_2)_n$-O-$(CH_2)_2$-CH_3 and CH_3-$(CH_2)_{10}$-CH_3 (1 Å=0.1 nm). (a) n=4, (b) n=7, (c) n=10, and (d) CH_3-$(CH_2)_{10}$-CH_3. See text.

oxygen atom in place of a carbon atom, the conformation of each chain changes. This leads to an increment of 0.8 Å in $\langle r \rangle$ and the MFE is enhanced by ca. 7%. The local conformation of a linker which connects two radicals may be also important in understanding MFEs.

The intensity ratio I_B/I_0 at 0.3 T for the fluorescence of

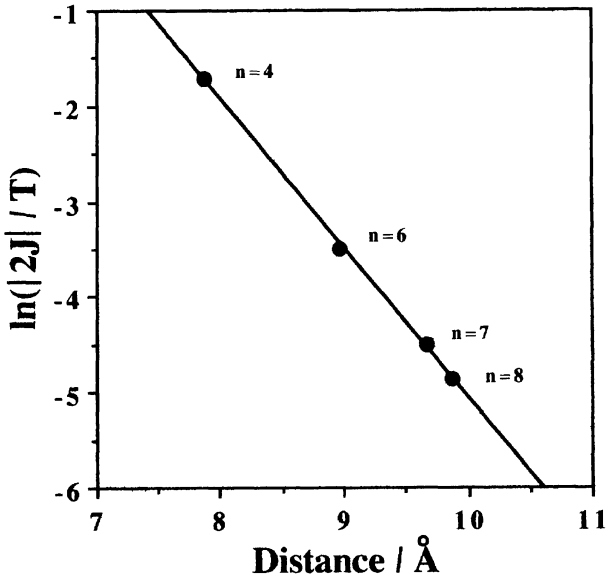

Fig. 16. Plot of ln $|2J|$ vs. $\langle r \rangle$. See text.

Py–$(CH_2)_{16}$–DMA is 1.6 in DMF,[4f] whereas that for the fluorescence of Phen-12-O-2-DMA is about 2.4 in DMF. The MFE in the former is about 70% of the value in the latter, though the total numbers of chain units in the former and the latter are 16 and 15, respectively. This means that the rate of the deactivation process from SE-SRIP, which is magnetic field independent, is faster in the former than in the latter, since the B_{av} values are nearly the same (both 5.5 mT), as discussed in a previous paper.[6a] The λ_{max}'s of the former and the latter exciplex fluorescence band are about 580 and 500 nm, respectively, indicating a smaller energy gap between the SE and its ground state in the former molecule. The nonradiative deactivation from SE-SRIP may be enhanced by the large Franck–Condon factor in the former.

2.2 Temperature Dependence of MFE: As shown in Fig. 12, the magnetic fields, where I_B/I_0 becomes a minimum (i.e., $|2J|$ value) of Phen-*n*-O-2-DMA (n=4,6,7), shift to a higher field with increasing temperature. It is considered that, with increasing temperature, the chain motion becomes faster and at the same time the mean distance between the two radical ions decreases. This is because trans form at methylene C–C bond is more stable than the gauche form by 2—3 kcal mol^{-1}, as is often discussed in polymer chemistry.[20] Staerk and his collaborators have examined theoretically and experimentally the mechanism of high-field shift of $|2J|$ of Py–$(CH_2)_n$–DMA, which is induced by solvent viscosity and temperature.[4b—4d] By decreasing solvent viscosity, $|2J|$ values for the molecules with n=7—16 shift to a high field. By increasing temperature, they also shift to a high field. The authors have concluded that a fast chain motion results in the high field shift of $|2J|$.

We attempted to examine the effect of temperature on $\langle r \rangle$, though the present observation, which is analogous to the reported one, may be partly explained in terms of the motional shift of $|2J|$. The MD calculation was, therefore, carried out for CH_3–$(CH_2)_4$–O–$(CH_2)_2$–CH_3 at two temperatures (223 and 333 K) (Table 3). The decrease in $\langle r \rangle$ is estimated to be about 0.3 Å between 223 and 333 K. When temperature dependence of $|2J|$ would be attributable solely to the shortening in the chain length, one could evaluate $\langle r \rangle$ by using the relationship of $|2J|$ and $\langle r \rangle$ shown in Fig. 16. From the $|2J|$ value of Phen-4-O-2-DMA shown in Fig. 12, the difference in $\langle r \rangle$ between 223 and 333 K is calculated to be 0.4 Å. This value agrees semiquantitatively with that obtained by the MD calculation. The high field shift of $|2J|$ values shown in Fig. 12 may be attributable partly to the contraction in the mean distance of the linker with temperature.

As shown in Fig. 12, the $|2J|$ value for the molecule with n=4 depends strongly on temperature, whereas those for n=6, 7 depend weakly on temperature. The degree of conformational freedom for the molecule with n=4 is much smaller than that for n=6,7, as shown in Fig. 15. By increasing temperature, a remarkable conformational change may take place in the former, whereas the change may be insignificant on average in the latter. This difference in the degree of conformational freedom may lead to the difference in the temperature dependence of $|2J|$ values.

Conclusions

MFEs on the exciplex fluorescence of Phen-*n*-O-2-DMA (n=4—12) have been studied as functions of solvent polarity, chain length, and temperature. The effects are interpreted in terms of the hf and S–T_- level crossing mechanisms of the radical ion pair, in which magnetic fields affect the S–T ISC of RIP which intervenes in the reaction. (1) Solvent dependence of the MFE on the exciplex fluorescence of Phen-10-O-2-DMA is discussed on the basis of the free energies of SE and SRIP. In THF (ε=7.6) the energy of the SRIP is slightly higher than that of exciplex, whereas in DMF (ε=36.7) the energy of SRIP is stabilized compared with that of SE. This results in the significant MFEs in DMF. (2) In DMF, the most significant effect on the exciplex fluorescence intensity ratio is observed for the long chain molecules (n=10,12) (ca. 2.2—2.4 times at 0.59 T). (3) The MFEs correlate strongly to the mean edge-to-edge distances $\langle r \rangle$ of two radical ions. S and T states of the RIP become nearly degenerate at $\langle r \rangle$=ca. 12 Å (n=10,12). (4) An experimental relationship between the exchange energy $|2J|$ and $\langle r \rangle$ is obtained: $2J=2J_0\exp(-\alpha\langle r \rangle)$, where $|2J_0|=4.014\times10^8$ G and $\alpha=1.566$ Å^{-1}. (5) It is suggested that the temperature-induced high-field shift of the $|2J|$ value for the molecule (n=4) is comparable with the magnitude which is expected from the thermal contraction of the linker.

H. C. thanks the Heiwa Nakajima Foundation for a scholarship. C.H.T. thanks the Japan Society for Promotion of Science for a fellowship. This work was partly supported by Grants-in-Aid Nos. 07NP0101, 07228248, 08218243 from the Ministry of Education, Science, Culture and Sports.

References

1) For recent reviews, see: a) U. E. Steiner and T. Ulrich, *Chem.*

Rev., **89**, 51 (1989); b) H. Hayashi, in "Photochemistry and Photophysics," ed by J. F. Rabek, CRC Press, Boca Raton (1990), Vol. 1, p. 59; c) U. E. Steiner and H.-J. Wolff, in "Photochemistry and Photophysics," ed by J. F. Rabek and G. W. Scott, CRC Press, Boca Raton (1991), Vol. IV, p. 1; d) K. Bhattacharya and M. Chowdhury, *Chem. Rev.*, **93**, 507 (1993); e) R. Nakagaki, Y. Tanimoto, and K. Mutai, *J. Phys. Org. Chem.*, **6**, 381 (1993); f) C. B. Grissom, *Chem. Rev.*, **95**, 3 (1995); g) A. L. Buchachenko, *Chem. Rev.*, **95**, 2507 (1995); h) Y. Tanimoto and Y. Fujiwara, *J. Synth. Org. Chem. Jpn.*, **53**, 413 (1995).

2) a) N. Kh. Petrov, A. I. Shushin, and E. L. Frankevich, *Chem. Phys. Lett.*, **82**, 339 (1981); b) N. Kh. Petrov, V. N. Borisenko, A. V. Starostin, and M. V. Alfimov, *J. Phys. Chem.*, **96**, 2901 (1992); c) N. Kh. Petrov, V. N. Borisenko, and M. V. Alfimov, *J. Chem. Soc., Faraday Trans.*, **90**, 109 (1994).

3) S. N. Batchelor, C. W. M. Kay, K. A. McLauchlan, and I. A. Shkrob, *J. Phys. Chem.*, **97**, 13250 (1993).

4) a) H. Staerk, W. Kühnle, R. Treichel, and A. Weller, *Chem. Phys. Lett.*, **118**, 19 (1985); b) H. Staerk, H.-G. Busmann, W. Kühnle, and A. Weller, *Chem. Phys. Lett.*, **155**, 603 (1989); c) H. Staerk, H.-G. Busmann, W. Kühnle, and R. Treichel, *J. Phys. Chem.*, **95**, 1906 (1991); d) H.-G. Busmann, H. Staerk, and A. Weller, *J. Chem. Phys.*, **91**, 4098 (1989); e) U. Werner, A. Wiessner, W. Kühnle, and H. Staerk, *J. Photochem. Photobiol.*, **A85**, 77 (1995); f) U. Werner and H. Staerk, *J. Phys. Chem.*, **99**, 248 (1995).

5) a) S. Basu, D. Nath, and M. Chowdhury, *J. Luminescence*, **40/41**, 252 (1988); b) S. Basu, D. N. Nath, M. Chowdhury, and M. A. Winnik, *Chem. Phys.*, **162**, 145 (1992); c) M. Chowdhury, R. Dutta, S. Basu, and D. Nath, *J. Mol. Liq.*, **57**, 195 (1993); d) R. Dutta, D. Nath, M. Chowdhury, and M. A. Winnik, *J. Photochem. Photobiol.*, **A84**, 265 (1994); e) S. Aich and S. Basu, *J. Chem. Soc., Faraday Trans.*, **91**, 1593 (1995).

6) a) Y. Tanimoto, N. Okada, M. Itoh, K. Iwai, K. Sugioka, F. Takemura, R. Nakagaki, and S. Nagakura, *Chem. Phys. Lett.*, **136**, 42 (1987); b) Y. Tanimoto, K. Hasegawa, N. Okada, M. Itoh, K. Iwai, K. Sugioka, F. Takemura, R. Nakagaki, and S. Nagakura, *J. Phys. Chem.*, **193**, 3586 (1989).

7) Y. Tanimoto, M. Takashima, and M. Itoh, *Bull. Chem. Soc. Jpn.*, **62**, 3923 (1989).

8) F. Guarnieri and W. C. Still, *J. Comput. Chem.*, **15**, 1302 (1994).

9) a) F. Mohamadi, N. G. J. Richards, W. C. Guida, R. Liskamp, M. Lipton, C. Caufield, G. Chang, T. Hendrickson, and W. C. Still, *J. Comput. Chem.*, **11**, 440 (1990); b) D. Q. McDonald and W. C. Still, *J. Am. Chem. Soc.*, **116**, 11550 (1994).

10) W. C. Still, A. Tempczyk, R. C. Hawley, and T. Hendrickson, *J. Am. Chem. Soc.*, **112**, 6127 (1990).

11) N. Christodouleas and W. H. Hamil, *J. Am. Chem. Soc.*, **86**, 5413 (1964).

12) G. J. Kavarnos, "Fundamental Concepts of Photoinduced Electron Transfer," Springer-Verlag, Berlin (1991).

13) H. Cao, K. Miyata, T. Tamura, Y. Fujiwara, Y. Tanimoto, M. Okazaki, K. Iwai, and M. Yamamoto, *Chem. Phys. Lett.*, **246**, 171 (1995).

14) H. Cao, Y. Fujiwara, A. Katsuki, C.-H. Tung, and Y. Tanimoto, *J. Phys. Chem.*, to be submitted.

15) Y. Tanimoto, unpublished work.

16) C. Herring and M. Flicker, *Phys. Rev.*, **A134**, 362 (1964).

17) H. Murai and K. Kuwata, *Chem. Phys. Lett.*, **164**, 567 (1989).

18) R. Kaptein, *J. Am. Chem. Soc.*, **94**, 6251 (1972).

19) F. J. J. de Kanter and R. Kaptein, *J. Am. Chem. Soc.*, **104**, 4759 (1982).

20) A. Abe, R. L. Jernigen, and P. J. Flory, *J. Am. Chem. Soc.*, **88**, 631 (1966).